

# Combined Diffusion and Perfusion MRI With Correlation to Single-Photon Emission CT in Acute Ischemic Stroke

## Ischemic Penumbra Predicts Infarct Growth

Jari O. Karonen, MD; Ritva L. Vanninen, MD, PhD; Yawu Liu, MD; Leif Østergaard, MD, MSc; Jyrki T. Kuikka, PhD; Juho Nuutinen, MD; Esko J. Vanninen, MD, PhD; P.L. Kaarina Partanen, MD, PhD; Pauli A. Vainio, PhD; Katja Korhonen, BM; Jussi Perkiö, MSc; Reina Roivainen, MD, PhD; Juhani Sivenius, MD, PhD; Hannu J. Aronen, MD, PhD

**Background and Purpose**—More effective imaging methods are needed to overcome the limitations of CT in the investigation of treatments for acute ischemic stroke. Diffusion-weighted MRI (DWI) is sensitive in detecting infarcted brain tissue, whereas perfusion-weighted MRI (PWI) can detect brain perfusion in the same imaging session. Combining these methods may help in identifying the ischemic penumbra, which is an important concept in the hemodynamics of acute stroke. The purpose of this study was to determine whether combined DWI and PWI in acute (<24 hours) ischemic stroke can predict infarct growth and final size.

**Methods**—Forty-six patients with acute ischemic stroke underwent DWI and PWI on days 1, 2, and 8. No patient received thrombolysis. Twenty-three patients underwent single-photon emission CT in the acute phase. Lesion volumes were measured from DWI, SPECT, and maps of relative cerebral blood flow calculated from PWI.

**Results**—The mean volume of infarcted tissue detected by DWI increased from 46.1 to 75.6 cm<sup>3</sup> between days 1 and 2 ( $P<0.001$ ;  $n=46$ ) and to 78.5 cm<sup>3</sup> after 1 week ( $P<0.001$ ;  $n=42$ ). The perfusion-diffusion mismatch correlated with infarct growth ( $r=0.699$ ,  $P<0.001$ ). The volume of hypoperfusion on the initial PWI correlated with final infarct size ( $r=0.827$ ,  $P<0.001$ ). The hypoperfusion volumes detected by PWI and SPECT correlated significantly ( $r=0.824$ ,  $P<0.001$ ).

**Conclusions**—Combined DWI and PWI can predict infarct enlargement in acute stroke. PWI can detect hypoperfused brain tissue in good agreement with SPECT in acute stroke. (*Stroke*. 1999;30:1583-1590.)

**Key Words:** magnetic resonance imaging, diffusion-weighted ■ penumbra ■ perfusion ■ stroke, acute ■ tomography, emission computed

Ischemic stroke is a common cause of death and disability in developed countries. Thrombolytic therapy with recombinant tissue plasminogen activator was shown to be effective in a selected subgroup of acute ischemic stroke patients.<sup>1</sup> According to the European Cooperative Acute Stroke Study (ECASS), patients receiving thrombolytic therapy should not have extensive ischemic changes on the initial CT scan.<sup>2</sup> Although CT can detect vasogenic edema in infarcted brain tissue in some cases within hours of the onset of symptoms,<sup>3</sup> conventional MRI is more sensitive.<sup>4,5</sup> However, since thrombolytic therapy must be given within a few hours of the onset of symptoms, the accuracy of both CT and conventional MRI in characterizing acute ischemic changes is not satisfactory.

Diffusion-weighted MRI (DWI) and perfusion-weighted MRI (PWI) are relatively new methods that can be utilized in

acute stroke imaging. DWI is based on the measurement of the diffusion of free water,<sup>6</sup> which is decreased in ischemic brain tissue.<sup>7,8</sup> DWI is very sensitive to infarcted brain tissue, which is seen as an area of high signal intensity compared with the signal from normal brain. This phenomenon can be investigated more quantitatively by studying the reduction in the apparent diffusion coefficient (ADC),<sup>9</sup> which has been detected in animals within minutes of the occlusion of the middle cerebral artery (MCA).<sup>10</sup> With PWI, hypoperfused tissue can be detected with the use of paramagnetic contrast agents, for example, gadolinium-based chelates.<sup>11,12</sup> On the basis of MR perfusion imaging data, maps of relative cerebral blood flow (rCBF) can be calculated.<sup>13,14</sup>

Single-photon emission CT (SPECT) is a well-characterized method for measuring cerebral blood flow (CBF), and its general availability makes it a potential tool in

Received March 12, 1999; final revision received May 11, 1999; accepted May 18, 1999.

From the Departments of Clinical Radiology (J.O.K., R.L.V., Y.L., P.L.K.P., P.A.V., K.K., H.J.A.), Clinical Physiology and Nuclear Medicine (J.T.K., E.J.V.), and Neurology (J.N., R.R., J.S.), Kuopio University Hospital (Finland); Department of Neuroradiology, Aarhus University Hospital (L.Ø.) (Denmark); and Department of Radiology, Helsinki University Central Hospital (J.P., H.J.A.) (Finland).

Reprint requests to Jari Karonen, MD, Department of Clinical Radiology, Kuopio University Hospital, PO Box 1777, FIN-70211 Kuopio, Finland. E-mail jari.karonen@kuh.fi

© 1999 American Heart Association, Inc.

Stroke is available at <http://www.strokeaha.org>

assessing acute ischemic stroke.<sup>15</sup> However, SPECT does not provide morphological information, and it may be logistically difficult to combine it with CT or MRI. Since PWI can be combined with DWI in a single imaging session, it could represent an alternative to SPECT in imaging brain perfusion. Experiences in detecting intraparenchymal hemorrhage with susceptibility-weighted MRI at 1.5 T seem promising,<sup>16,17</sup> which may support the potential role of MRI as the primary imaging tool in acute stroke.

The target of novel therapeutic approaches is the ischemic penumbra, where the hypoperfused brain tissue is functionally impaired but salvageable if perfusion is restored.<sup>18</sup> If the volume of hypoperfused tissue differs from the volume of tissue with decreased diffusion (perfusion-diffusion mismatch), this volume difference may be used as an estimate of the ischemic penumbra. The ischemic penumbra may also be estimated in terms of the absolute CBF relative to the ischemic limit.<sup>19</sup>

The purpose of the present study was to evaluate the potential of combined DWI and PWI in acute (<24 hours) ischemic stroke to predict infarct growth and final infarct size. We studied this by comparing initial infarct volume with the volume of hypoperfused tissue and by correlating the size of this perfusion-diffusion mismatch to the subsequent change in infarct volume. In addition, our aim was to compare PWI with SPECT, which is a well-established method used to measure CBF.

### Subjects and Methods

Forty-six consecutive patients (21 men, 25 women; mean age, 72 years; age range, 48 to 89 years) presenting with symptoms indicative of acute supratentorial ischemia were prospectively enrolled into the study. They were selected from a nonuniform patient population with a wide range of neurological symptoms admitted to the neurological emergency department of our university hospital. CT was performed on all patients to exclude hemorrhage and other nonischemic causes of the symptoms, which were exclusion criteria. Twenty-five patients had left-sided motor deficit and 21 had right-sided motor deficit, 10 of them with dysphasia or aphasia.

The first MRI was performed as soon as possible after the patient's admission to the hospital. The time delay from the CT examination to the first MRI was  $3.0 \pm 2.6$  (mean  $\pm$  SD) hours. If the patient could not undergo the first MRI within 24 hours of the onset of symptoms or the time when he or she was last seen healthy, the patient was excluded from the study. The first MRI (n=46) was performed  $9.9 \pm 5.4$  hours, the second MRI (n=46)  $30.7 \pm 6.7$  hours, and the third MRI (n=42) 7.1 days  $\pm$  16 hours after the onset of symptoms. Patients with general contraindications to MRI (eg, cardiac pacemakers, claustrophobia) were excluded as well as patients who were too unstable for MRI. The second MRI was performed on day 2, and the third MRI was performed 1 week after the onset of symptoms. Twenty-three of 46 patients also underwent SPECT in the acute phase, 14 of them on day 1 and 9 of them on day 2 after the onset of symptoms.

No patient received experimental neuroprotective agents, but 1 patient received placebo as part of the ECASS II trial.<sup>20</sup> No patient was treated with thrombolysis. Two patients were treated with intravenous heparinoid as part of the Euro-TOAST (Trial of Org 10172 in Acute Stroke Treatment) study protocol. Five patients were treated with intravenous heparin for stroke progression, and 6 patients with cardioembolic stroke were treated with warfarin. Other patients were treated with aspirin with or without dipyridamole and received standard supportive therapy for acute ischemic stroke.

Informed consent was obtained from the patient or the patient's relative. The study design was approved by the ethics committee of our institution.

### Evaluation of CT Findings

Ischemic CT findings were not an exclusion criterion. They were categorized as follows: (1) no acute ischemic findings, (2) subtle ischemic findings, and (3) definite ischemic findings. Detailed comparison of CT and MRI findings was not performed because of the time delay between CT and MRI.

### MRI Protocol

Each MRI examination consisted of DWI, PWI, and conventional imaging. The total imaging time was approximately 20 minutes. All MRI examinations were performed with a 1.5-T echo-planar imaging (EPI)-capable whole body scanner (Magnetom Vision, Siemens Medical Systems) with the use of a head coil and standard restraints.

DWI was performed with an EPI spin-echo sequence (repetition time, 4000 milliseconds; echo time, 103 milliseconds). Nineteen axial slices tilted along the orbitomeatal line covering the whole supratentorial brain were imaged (slice thickness, 5 mm; interslice gap, 1.5 mm; field of view, 260 mm; matrix size,  $96 \times 128$  interpolated to  $256 \times 256$ ; acquisition time, 20 seconds). A T2-weighted reference image (b value, 0 s/mm<sup>2</sup>) and 3 diffusion-weighted images with orthogonally applied diffusion gradients (b value, 1000 s/mm<sup>2</sup>) were collected.

Perfusion imaging also used an EPI spin-echo sequence (repetition time, 1500 milliseconds; echo time, 78 milliseconds) and was targeted to the central area of ischemia. Seven axial slices (slice thickness, 5 mm; interslice gap, 1.5 mm; field of view, 260 mm; matrix size,  $116 \times 256$ ) were acquired. The positions and tilt of the slices were set to match the 7 slices on DWI that contained the largest diffusion defects. The 7 slices were imaged 40 times every 1.5 seconds, with a total imaging time of 1 minute. Before the injection of contrast medium, 4 sets of baseline images were collected. More baseline images resulted from the time delay between the intravenous injection of the contrast medium and its arrival to the cerebral arterial circulation. Gadopentetate dimeglumine (Magnevist, Schering AG; 0.2 mmol/kg body wt) was injected into the antecubital vein with an 18-gauge cannula. The injection was performed at a speed of 5 mL/s with an MR-compatible power injector (Spectris, Medrad). The bolus of contrast medium was followed by a 15-mL bolus of saline at the same injection rate. Because DWI and conventional imaging were performed before PWI, the intravenous line was kept open by flushing it with 0.25 mL of saline per minute.

### SPECT Imaging Protocol

Technetium-99m ethyl cysteinate dimer was used as the tracer<sup>21</sup> and prepared according to the manufacturer's instructions (DuPont Pharma/Durham APS). A dose of 550 to 720 MBq, depending on the body weight of the patient, was injected into the antecubital vein before or after the MRI examination. The time delay between MRI and injection of the tracer was limited to 1 hour to achieve temporally comparable findings in PWI and SPECT. Within 60 minutes of the injection, the high-resolution SPECT acquisition was performed with a gamma camera equipped with fan-beam collimators (MultiSPECT 3, Siemens Medical Systems, Inc). A full 360° rotation was acquired (40 views per detector, each for 35 seconds) with  $128 \times 128$  pixels in resolution. Along the orbitomeatal line tilted contiguous transaxial and coronal slices (2 pixels in width; 6 mm) were reconstructed by filtered backprojection and corrected for attenuation. The imaging resolution was 8 to 9 mm.<sup>22</sup>

### Postprocessing of the Imaging Data

To minimize the effects of diffusion anisotropy, trace images (trace of the diffusion tensor) were generated by calculating the average of the 3 diffusion-weighted images.<sup>23,24</sup> ADC maps were calculated on a pixel-by-pixel basis. The calculation of ADC was based on the negative slope of the line fitting the 2 points for b versus  $\ln(SI)$ ,

where SI is signal intensity. Volumes of decreased diffusion were measured by drawing regions of interest (ROIs) around the lesions on the trace images and by multiplying the lesion area by the slice thickness. The tracings were shared between 2 interpreters (J.O.K. and Y.L.) blinded to the clinical data. ADC maps were reviewed to rule out the effects of T2 shine-through, which would have in some cases caused overestimation of infarcted tissue. The interslice gap was estimated to contain a lesion of the same size as the slice above it, and the lesion inside the gap was included in the volume calculation.

Perfusion raw images were transferred to a UNIX workstation (Sun SPARC Ultra) for calculation of rCBF maps. Tissue and arterial contrast agent levels were determined with the assumption of a linear relationship between transverse relaxivity ( $\Delta R_2$ ) and intravascular concentration of Gd-DTPA.<sup>11,25,26</sup> The shape of the arterial input function was determined from a few pixels located at 1 branch of the MCA, showing large signal losses during the bolus passage. In each imaging pixel, the tissue concentration-time curve was deconvolved with the arterial input function to determine the tissue impulse response. CBF was subsequently determined as the height of the deconvolved tissue impulse response.<sup>13,14</sup>

The volume of decreased perfusion was determined visually by 1 interpreter (J.O.K.) by drawing a ROI around the pathological area slice by slice. A commercially available image analysis software package was used (Cheshire, Perceptive Systems, Inc). After the ROIs were multiplied by the slice thickness of 5 mm and the interslice gaps, they were summed to give the total volume of hypoperfused tissue in the 7 imaged slices. However, the lesion area in the lowermost lesion-containing slice was multiplied only by the slice thickness but not by the gap thickness. Because an acute hypoperfusion could not be distinguished from probable old perfusion defects, the interpreter was not blinded to the diffusion imaging findings but was blinded to the clinical data of the patients.

To test the interobserver variability in the measurements, 2 observers (J.O.K. and Y.L.) independently drew ROIs in 80 trace images and 70 rCBF maps of 10 randomly selected patients. To test intraobserver reproducibility, 1 of the observers performed the measurements twice in 5 randomly selected patients, with an interval of at least 6 months between measurements.

A semiautomatic brain quantification program (Siemens Medical Systems, Inc) was used to analyze the size of the perfusion defect on SPECT. The perfusion defect was defined as cortical regions with count rates <60% of the maximal cortical rate. The ROIs were manually drawn onto the consecutive slices by an experienced rater who was not aware of the PWI findings or the clinical status of the patient. However, the rater was aware of the DWI findings to be able to differentiate between acute and chronic perfusion defects on SPECT.

## Volumetrics

The total infarct volume was measured from all DWI slices containing the lesion. Because of the limited number of slices in perfusion imaging, the true volume of hypoperfusion could not be entirely measured in 23 cases of larger infarctions. In those cases, the volumes of decreased diffusion were also calculated from the 7 slices corresponding to the slices in perfusion imaging.

The following volumes were measured: (1) total volume of tissue with decreased diffusion; (2) volume of hypoperfused tissue in rCBF maps in the 7 slices included in PWI; (3) volume of tissue with decreased diffusion limited to the 7 slices comparable to PWI of the same day; (4) volumes of decreased diffusion on day 2 and at 1 week from the same slice positions where PWI was performed on day 1 to compare the same tissue volume when infarct growth and final infarct size were considered; and (5) volumes of hypoperfused tissue on SPECT calculated from the same 7 slices corresponding to the area of PWI on the same day. The contiguous slices on SPECT were 6 mm thick, causing a slight inconsistency compared with seven 5-mm-thick PWI slices with 1.5-mm gaps.

The perfusion-diffusion mismatch was calculated by subtracting the DWI lesion volume from the hypoperfusion volume in rCBF maps. Infarct growth was defined as the increase in infarcted tissue

volumes measured from the DWI slices matching the positions of the 7 slices on the initial PWI.

## Assessment of the Neurological Status of the Patient

The mean National Institutes of Health Stroke Scale (NIHSS)<sup>27</sup> was measured by a neurologist (J.N., R.R., or J.S.) on day 1 and at 1 week. The initial mean NIHSS score was  $12.4 \pm 8.1$  (mean  $\pm$  SD), ranging from 0 (no symptoms measured by the NIHSS) to 38.

## Statistical Analysis

Since there was a significant deviation from normal distribution, nonparametric tests were used to test the significance of volume differences. The significance of changes in mean infarct volumes and the differences between infarct volumes and hypoperfusion volumes were tested with the Wilcoxon matched-pairs signed rank test. The Spearman correlation coefficient was used to calculate (1) correlation between hypoperfusion volumes in PWI maps and SPECT, (2) correlation between perfusion-diffusion mismatch and infarct growth, (3) correlation between initial hypoperfusion volume in PWI maps and infarct size at 1 week, and (4) interobserver variability and intraobserver reproducibility by 2 measurers for measured DWI and PWI for both lesion area (slice by slice) and lesion volume (patient by patient).

Furthermore, the patient population was divided into 2 groups according to the perfusion-diffusion mismatch: group 1, ratio of PWI lesion volume to DWI lesion volume <1.10; and group 2, ratio of PWI lesion volume to DWI lesion volume  $\geq 1.10$ . After this dichotomization, the Mann-Whitney *U* test was used to test whether the change in the NIHSS score during the week differed significantly between groups 1 and 2. The Mann-Whitney *U* test was also used to test whether the anticoagulant treatment with warfarin or intravenous heparin was associated with infarct growth during the week. A *P*-value <0.05 was considered statistically significant. Statistical analysis was performed with a statistical software package (SPSS Win 7.5, SPSS Inc).

## Results

On CT, 22 patients (48%) did not have ischemic findings, 10 patients (22%) had subtle ischemic findings, and 14 patients (30%) had definite ischemic findings. All patients had definite acute ischemic findings on DWI: 21 patients (46%) had their infarct in the left hemisphere and 25 patients (54%) in the right hemisphere.

Four of 46 patients did not undergo the third MRI (3 died, 1 refused). DWI was successfully completed in every MRI. The hypoperfusion volume in PWI was not available in 8 cases on the first day (because of patient motion [*n*=5], malfunction of the scanner [*n*=1], or operator-dependent error [*n*=2]). Hypoperfusion volume in PWI was not available in 13 cases on day 2 (patient motion [*n*=6], serious imaging artifact [*n*=4], or operator-dependent error [*n*=3]) and in 3 cases at 1 week (malfunction of the scanner [*n*=2], operator-dependent error [*n*=1]). PWI was thus successfully performed on 38 patients on day 1, on 33 patients on day 2, and on 39 patients at 1 week.

The mean volume of infarcted tissue measured from the diffusion trace images increased from  $46.1 \text{ cm}^3$  (*n*=46) on day 1 to  $75.6 \text{ cm}^3$  on day 2 (*n*=46; *P*<0.001). When measured at 1 week, the mean infarct volume had still slightly increased to  $78.5 \text{ cm}^3$  (*n*=42; *P*<0.001) (Table 1). A representative case showing the infarct growth is presented in Figure 1.



**TABLE 1. Mean Lesion Volumes on DWI During the Week After the Onset of Stroke Symptoms**

	n	Lesion Volume on DWI, cm <sup>3</sup>		Growth of Lesion on DWI, cm <sup>3*</sup>	
		Mean±SD	Range	Mean	P†
Day 1	46	46.1±68.8	0.1–385.3		
Day 2	46	75.6±103.0	0.6–555.6	29.5	<0.001
Week 1	42	78.5±92.0	0.2–379.5	2.9	<0.001

\*Growth of lesion compared with lesion size on previous DWI.

†Indicates significance of growth of the lesion (Wilcoxon matched-pairs signed rank test).

The volumes of hypoperfused tissue on PWI compared with the volume of infarcted tissue measured from the corresponding DWI slices are presented in Table 2. On day 1, the infarcted tissue was not totally covered by 7 slices in 23 patients. The mean volume of infarcted tissue outside the 7 slices was 15.8 cm<sup>3</sup>. On day 1, the hypoperfusion volume on rCBF maps was significantly greater than the infarct volume on DWI ( $P<0.001$ ). On day 2, the hypoperfusion volume was still greater than the infarct volume ( $P=0.014$ ). At 1 week, the hypoperfusion volume had decreased and was actually smaller than the infarct volume on DWI. This is probably due to reperfusion in the infarcted tissue, and in a few cases findings suggesting hyperperfusion were detected.

The perfusion-diffusion mismatch correlated statistically significantly with infarct growth between days 1 and 2

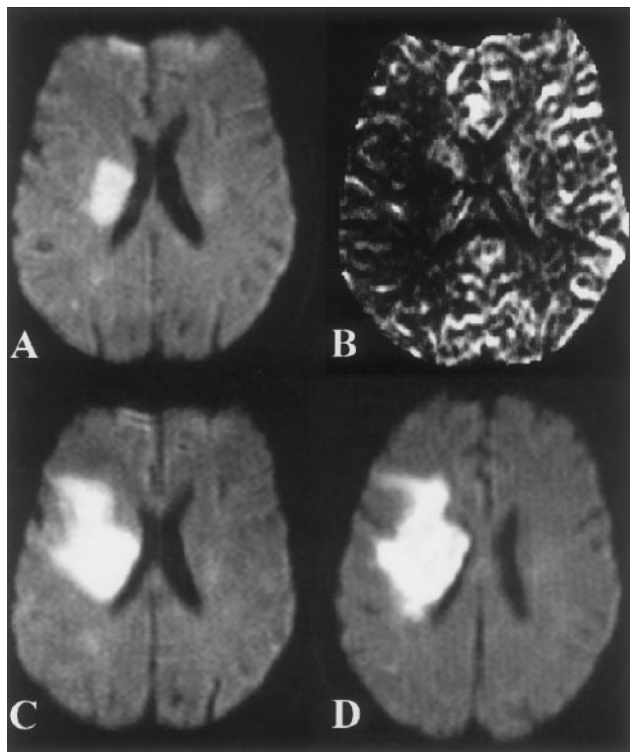


**Figure 1.** A 73-year-old woman with left hemiparesis. The first MRI was performed 6 hours after the onset of symptoms. In this first imaging, the bright area in the trace image (A) representing the infarct is clearly smaller than the hypoperfusion area on the rCBF map (B). Infarct growth is demonstrated on the diffusion-weighted trace images 27 hours (C) and 1 week (D) after the onset of symptoms.

**TABLE 2. Mean Lesion Volumes on 7 Corresponding DWI and PWI Slices During the Week After the Onset of Stroke Symptoms**

	n	Lesion Volume on DWI, cm <sup>3</sup>		Hypoperfusion Volume on PWI, cm <sup>3</sup>	
		Mean±SD	Mean±SD	Mean±SD	P*
Day 1	38	34.6±50.4	82.8±74.1		<0.001
Day 2	33	56.8±70.8	73.5±76.3		0.014
Week 1	39	63.2±64.8	51.4±72.0		0.063

Volume measurements on DWI were performed from slices corresponding to the 7 slices included on PWI. \*Indicates significance of the size difference between hypoperfusion volume and lesion volume on DWI (Wilcoxon matched-pairs signed rank test).

( $r=0.586$ ,  $P<0.001$ ;  $n=38$ ) and between day 1 and 1 week ( $r=0.699$ ,  $P<0.001$ ;  $n=34$ ). A typical case in which the perfusion-diffusion mismatch detects tissue at risk, part of which eventually proceeds to infarction, is shown in Figure 1. A case with absence of perfusion-diffusion mismatch on day 1 and no significant infarct growth is shown in Figure 2. The hypoperfusion volume measured from rCBF maps on day 1 correlated statistically significantly with the final infarct size measured from DWI at 1 week after the onset of symptoms ( $r=0.827$ ,  $P<0.001$ ;  $n=34$ ).

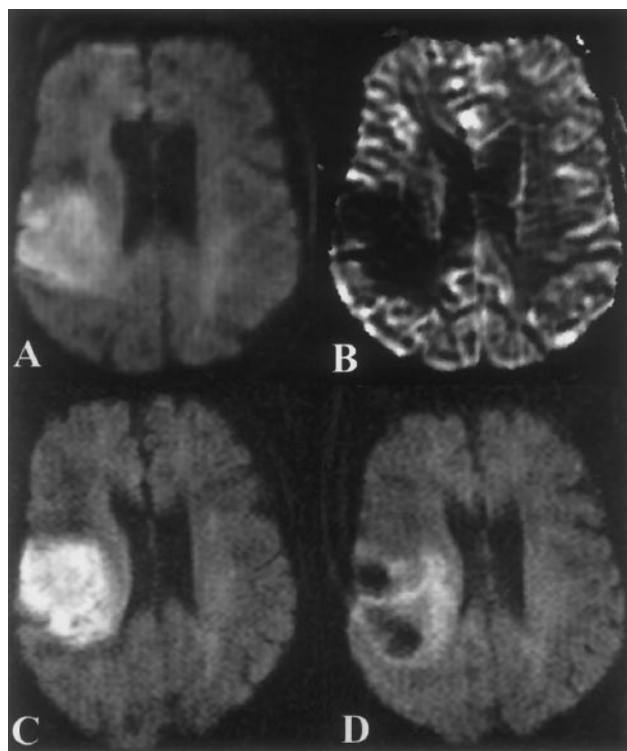


**Figure 2.** A 71-year-old man with left hemiparesis. A hyperintense lesion representing infarction is detected on diffusion-weighted trace image 15 hours (A) after the onset of symptoms. At the same time, PWI (B) shows a hypoperfusion area that is not significantly larger than the infarct. No significant growth is seen in the infarct, as demonstrated by diffusion-weighted trace images 39 hours (C) and 1 week (D) after the onset of symptoms. Note the hemorrhagic transformation at 1 week in D, visible as dark regions because of the susceptibility effect of the breakdown products of hemoglobin.

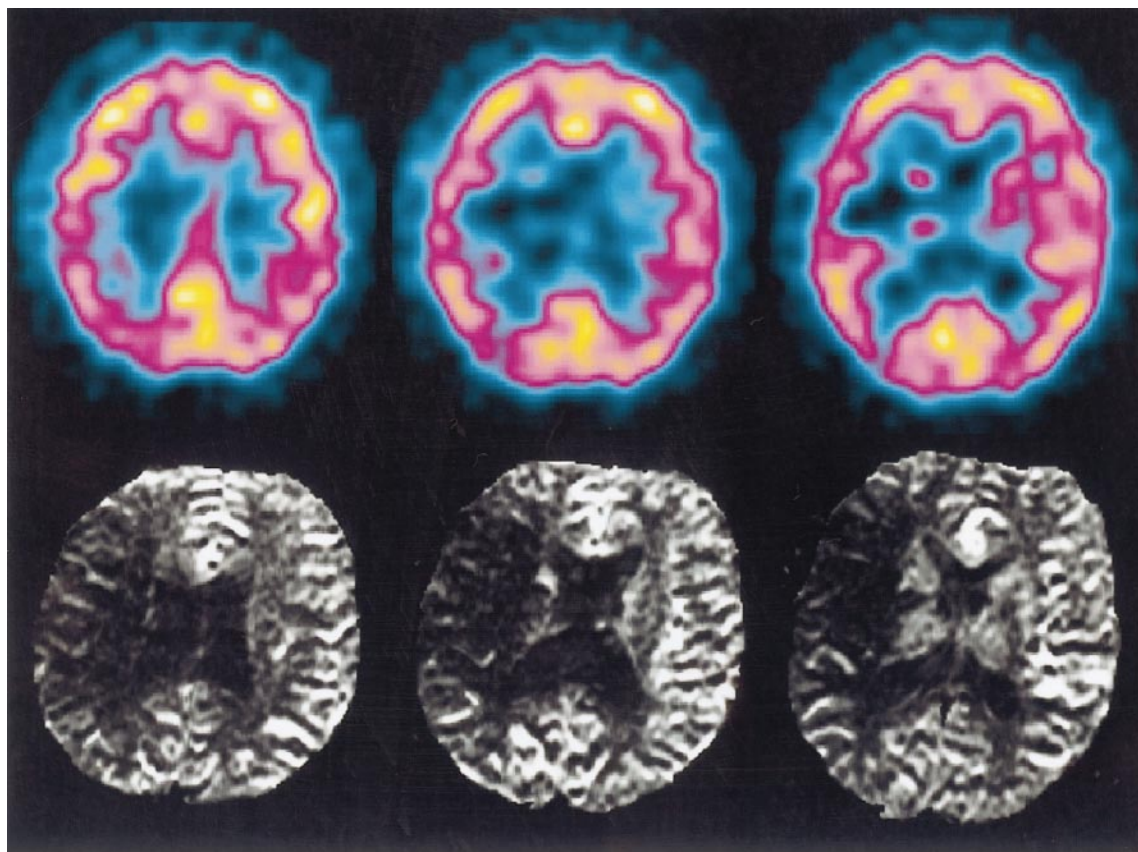


**Figure 3.** A 56-year-old man with left hemiparesis. Top, Three contiguous slices on SPECT, which detect hypoperfusion in the right hemisphere. Bottom, Corresponding slices on the rCBF maps, demonstrating the similarity of the findings on PWI and SPECT, which is a well-characterized method to measure brain perfusion. The MR perfusion study was performed 9.5 hours after the onset of symptoms. The findings on SPECT and PWI can be considered temporally well comparable, because the tracer injection for SPECT was given approximately 20 minutes before the MR perfusion study.

The hypoperfusion volume on SPECT in the acute phase (mean,  $82.5 \pm 124.8 \text{ cm}^3$ ) correlated strongly with the hypoperfusion volume measured from rCBF maps (mean,  $79.2 \pm 78.3 \text{ cm}^3$ ) on the same day ( $r=0.824$ ,  $P<0.001$ ;  $n=23$ ). Note that these mean volumes result from the PWI of day 1 or 2, depending on the day when SPECT was performed. Figure 3 shows a comparison of PWI with SPECT.

Infarct growth during the week in patients receiving anticoagulant treatment did not differ significantly ( $P=0.81$ ) from infarct growth in patients not receiving anticoagulant treatment.

In interobserver variability analysis, the DWI lesion areas measured slice by slice correlated well between the 2 measurers ( $r=0.964$ ,  $P<0.01$ ;  $n=80$  slices). The hypoperfusion areas measured from rCBF maps slice by slice also correlated well between 2 measurers ( $r=0.907$ ,  $P<0.01$ ;  $n=70$  slices) (Figure 4). When lesion volumes were calculated patient by patient, the correlations between volumes measured by 2 measurers were also significant for DWI ( $r=0.976$ ,  $P<0.01$ ;  $n=10$ ) and PWI ( $r=0.976$ ,  $P<0.01$ ;  $n=10$ ).

In intraobserver reproducibility analysis, the correlation of 2 measurements slice by slice was significant for DWI ( $r=0.950$ ,  $P<0.01$ ;  $n=40$  slices) and PWI ( $r=0.802$ ,  $P<0.01$ ;  $n=35$  slices).

During the week, the mean NIHSS score changed from  $12.4 \pm 8.1$  to  $9.3 \pm 9.6$ , when 3 patients had died. The NIHSS

score change did not differ significantly ( $P=0.52$ ) between groups 1 (ratio of PWI to DWI  $<1.10$ ;  $n=7$ ) and 2 (ratio of PWI to DWI  $\geq 1.10$ ;  $n=28$ ). Three patients who died were excluded from the analysis because death is not coded in the NIHSS. However, they all had perfusion-diffusion mismatch ratio  $>1.10$ . In group 2, the perfusion-diffusion mismatch was  $59.2 \pm 49.1 \text{ cm}^3$ . In group 1, the perfusion-diffusion mismatch was  $-0.4 \pm 2.5 \text{ cm}^3$ .

## Discussion

In previous studies, DWI has been shown to be an efficient method in the diagnosis of acute ischemic stroke.<sup>9,28,29</sup> Experimental animal work has shown that lesions with decreased diffusion can partly recover if perfusion is restored after 1 hour from occlusion of the MCA.<sup>30</sup> Although detection of the ischemic penumbra with DWI alone seems tempting, it has not yet been possible.<sup>31</sup> In humans, only a few observations of reversibility of ischemic lesions with decreased diffusion have been made.<sup>32-34</sup> When one considers the speculations of rare reversibility of DWI findings in humans, it is obvious that DWI is at present the most accurate clinically available method to visualize infarcted brain tissue.

Because DWI at present cannot totally characterize the hemodynamics of the ischemic process, other groups have also used combined DWI and PWI to distinguish the ischemic

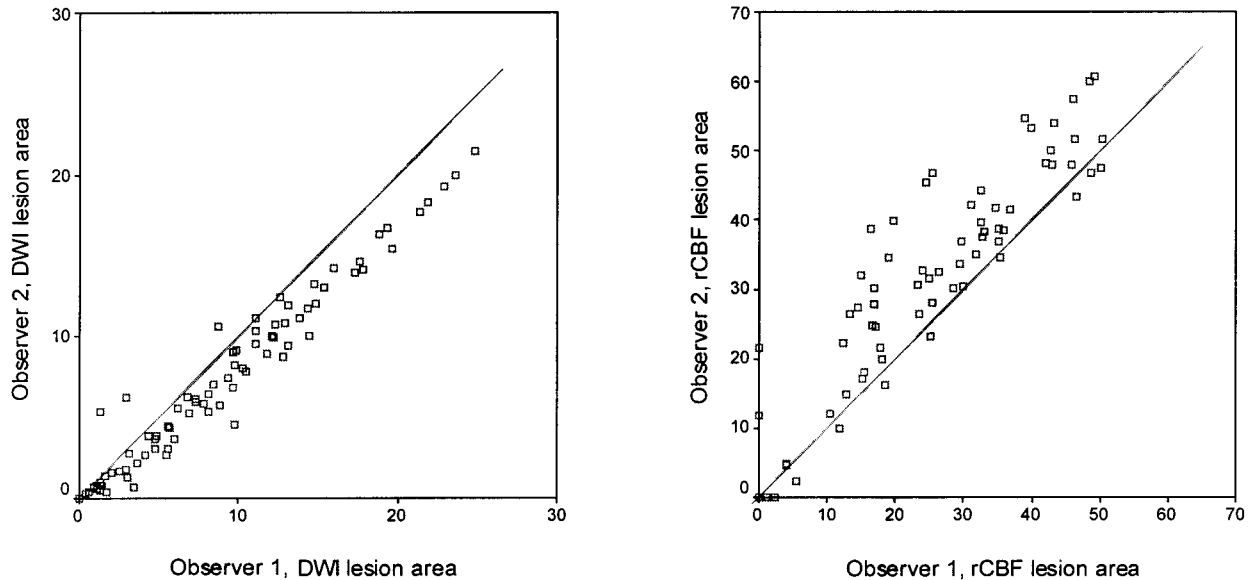


**Figure 4.** Interobserver variability for DWI lesion areas ( $r=0.964$ ) (left) and rCBF lesion areas ( $r=0.907$ ) (right) slice by slice (unit:  $\text{cm}^2$ ).

penumbra from permanently damaged tissue. In this approach, perfusion-diffusion mismatch is used to estimate the presence and size of the ischemic penumbra. Warach et al<sup>35</sup> first demonstrated the ability of combined DWI and single-slice PWI to predict clinical outcome. In the series of Sorensen et al,<sup>34</sup> the lesion on DWI was generally smaller than the hypoperfusion volume in maps of relative cerebral blood volume. Baird et al<sup>36</sup> detected, in a subgroup of 13 patients, that perfusion-diffusion mismatch (mean transit time as the perfusion parameter) in the acute phase may be predictive of infarct growth. Rordorf et al<sup>37</sup> observed that the infarct more often showed progression into the surrounding hypoperfused tissue (detected by maps of relative cerebral blood volume) if there was a MCA stem occlusion on MR angiography. Tong et al<sup>38</sup> demonstrated a correlation of lesion volumes on DWI and PWI (maps of time to peak) with clinical status after 24 hours and infarct size at 1 week. Barber et al<sup>39</sup> detected that perfusion-diffusion mismatch (relative mean transit time as the perfusion parameter) predicted DWI lesion growth.

We were able to perform DWI in all 46 patients and PWI in 38 of 46 patients (83%) in the acute phase of ischemic stroke. Patient movement or lack of cooperation was responsible for 5 of 8 failures of PWI. We conclude that DWI and PWI can be performed in the routine diagnosis of acute stroke.

There was good agreement between volumes of decreased rCBF measured by SPECT and PWI. Lesions that were apparently small on SPECT were somewhat larger on PWI, probably because of the difference in resolution of these techniques (Figure 5).

We performed the third MRI after 1 week from the onset of stroke to establish the final size of the infarct. The initial hypoperfusion volumes in rCBF maps showed good correlation with the infarct size at 1 week (Figure 6). CBF begins to change only when cerebral perfusion pressure falls below the range of normal autoregulation, ie, when hypoperfusion is

severe. One would therefore expect decreased CBF to be clearly associated with a high risk of subsequent infarction. Figure 7 shows perfusion-diffusion mismatch versus lesion growth on DWI during the week. Note that hypoperfusion volume on the rCBF map is usually larger than the tissue that eventually proceeds to infarction (Figure 6). Even though there is a decrease in CBF, neuronal function is maintained until CBF falls below a relatively fixed threshold ( $\approx 20$  mL/100 g per minute). Below this threshold, survival time is limited. We therefore speculate that future risk assessments based on the degree of rCBF deficit (relative to white matter flow rates, for example) and the duration of ischemia might possibly improve the predictive value of rCBF maps.

rCBF maps seem to be accurate prognostic markers in demonstrating tissue at risk. However, one should take into account the time from the onset of symptoms, since the brain tissue is able to survive decreased blood flow only for a

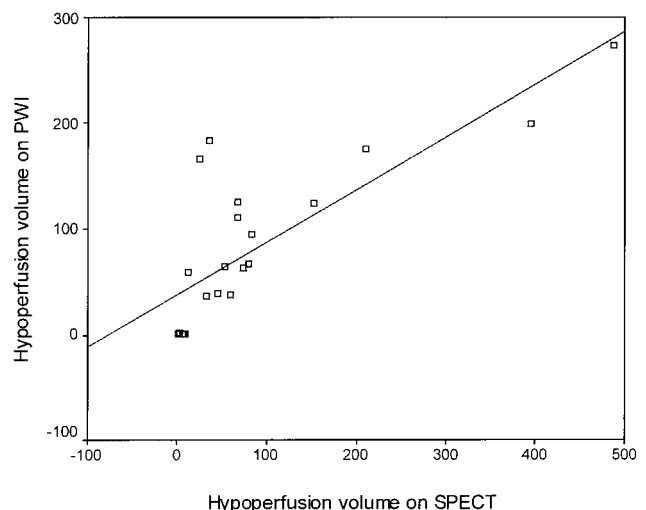


**Figure 5.** Correlation of hypoperfusion volume measured from rCBF maps with hypoperfusion volume measured from SPECT.



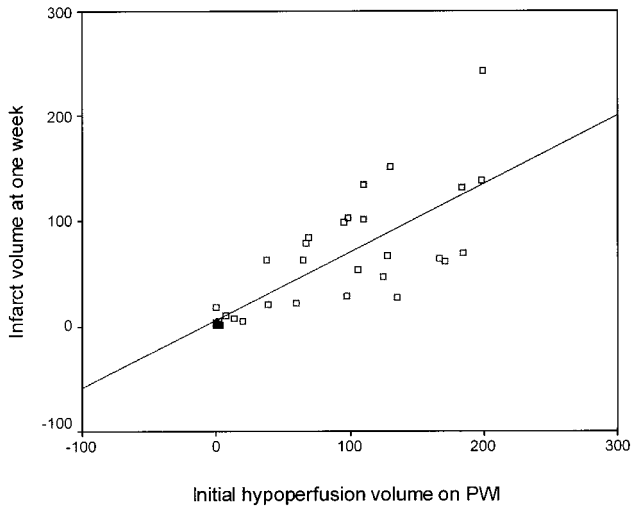


**Figure 6.** Correlation of hypoperfusion volume on day 1 with infarct size on DWI at 1 week. Hypoperfusion volume was measured from rCBF maps calculated on the basis of PWI on day 1.

relatively short time. In this study we used perfusion-diffusion mismatch as a tool to estimate the ischemic penumbra. Other hypotheses regarding how the ischemic penumbra could be estimated in a patient also exist, for example, by measuring absolute CBF.

There are certain limitations in our study. The patients did not receive thrombolytic treatment, but we think that this makes our material fairly representative of the natural course of ischemic stroke during the first week after stroke onset. Anticoagulant treatment did not affect infarct growth. The data presented here are not confounded by reperfusion other than what may have occurred spontaneously.

Spin-echo PWI, which is sensitive to microvascular perfusion, could be performed in only 7 slices to maintain the temporal resolution of 1.5 seconds between the measure-

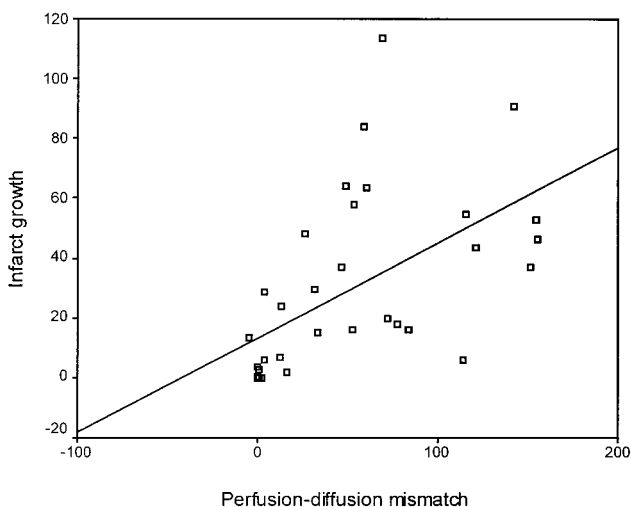


**Figure 7.** Correlation of perfusion-diffusion mismatch on day 1 with infarct growth during the first week after the onset of symptoms. Infarct growth was defined as the volume difference between the lesions on DWI on day 1 and after 1 week. For calculation of perfusion-diffusion mismatch, hypoperfusion volume was measured from rCBF maps calculated on the basis of PWI on day 1.

ments. We imaged a representative sample of the infarct to be covered with PWI by matching the middle PWI slice with the DWI slice containing the largest diffusion defect. This slice was in most cases located in the center of the infarct but, because the infarct can expand in any direction, the imaged areas in PWI are not strictly comparable.

There was a large variation in infarct size in this population, and patients were selected from a patient population with different neurological symptoms. Patient recruitment was partly simultaneous with the ECASS II trial,<sup>20</sup> and 1 patient received placebo before the first MRI. Otherwise, patients were not considered for thrombolysis because it is not an approved treatment for acute ischemic stroke at our hospital, and the majority of patients were admitted to the hospital >3 hours from the onset of symptoms. We believe that our patient population is representative and reflects the reality in most clinical institutions at present.

Our results show that the infarct enlarges between days 1 and 2, which is in agreement with the study of Baird et al.<sup>36</sup> This supports the view that there could be a place for the use of neuroprotective agents later than only a few hours from the onset of symptoms. Although neuroprotection has been beneficial in experimental stroke in animals, no neuroprotective agent has yet proved effective in humans.<sup>40</sup> The dynamic nature of the ischemic penumbra and different mechanisms of potential treatments have questioned the concept of a universal narrow time window.<sup>41</sup>

Hypoperfusion on rCBF maps correlated well with hypoperfusion on SPECT images (Figure 5). Unlike SPECT, our MR method allows direct visualization of irreversibly damaged tissue by DWI. In clinical management, thrombolytic treatment is potentially hazardous in patients with large infarcts,<sup>1</sup> giving the integrated MR examination a potential advantage in clinical decision making.

The present study is based on a prospective series of acute stroke patients imaged repeatedly with a uniform MRI protocol. The patients did not receive thrombolytic treatment, and therefore the results reflect the natural history of acute ischemic stroke. CT was performed initially as part of the clinical routine, and SPECT was used as a reference method for MR perfusion imaging. We conclude that combined DWI and PWI can be used in estimating the presence and the size of the penumbra in acute nonhemorrhagic ischemic stroke. The penumbra on day 1, estimated as perfusion-diffusion mismatch, correlates statistically significantly with the growth of infarct detected as an increase in the volume of decreased diffusion. Finally, hypoperfusion volume on rCBF maps correlated significantly with final infarct size at 1 week. The combination of DWI and PWI is a powerful tool to predict and follow the course of acute ischemic stroke.

## Acknowledgments

This study was supported by Kuopio University Hospital (EVO funding 307/97 and 21/98), the Radiological Society of Finland, the Instrumentarium Science Foundation, the Aarne Koskelo Foundation, and the Paavo Nurmi Foundation. We thank Helena Kiiliäinen for ROI analysis of SPECT images and Timo Voivalin, Tuula Bruun, and Mervi Könönen for technical and secretarial assistance.

## References

1. The National Institute of Neurological Disorders and Stroke rt-PA Stroke Study Group. Tissue plasminogen activator for acute ischemic stroke. *N Engl J Med*. 1995;333:1581–1587.
2. Hacke W, Kaste M, Fieschi C, Toni D, Lesaffre E, von Kummer R, Boysen G, Bluhmki E, Hoxter G, Mahagne MH, Hennerici M. Intravenous thrombolysis with recombinant tissue plasminogen activator for acute hemispheric stroke: the European Cooperative Acute Stroke Study (ECASS). *JAMA*. 1995;274:1017–1025.
3. von Kummer R, Allen KL, Holle R, Bozzao L, Bastianello S, Manelfe C, Bluhmki E, Ringleb P, Meier DH, Hacke W. Acute stroke: usefulness of early CT findings before thrombolytic therapy. *Radiology*. 1997;205:327–333.
4. Bryan RN, Levy LM, Whitlow WD, Killian JM, Preziosi TJ, Rosario JA. Diagnosis of acute cerebral infarction: comparison of CT and MR imaging. *AJNR Am J Neuroradiol*. 1991;12:611–620.
5. Yuh WT, Crain MR, Loes DJ, Greene GM, Ryals TJ, Sato Y. MR imaging of cerebral ischemia: findings in the first 24 hours. *AJNR Am J Neuroradiol*. 1991;12:621–629.
6. Stejskal EO, Tanner JE. Spin diffusion measurements: spin echoes in the presence of a time-dependent field gradient. *J Chem Phys*. 1965;42:288–292.
7. Le Bihan D, Breton E, Lallemand D, Grenier P, Cabanis E, Laval-Jeantet M. MR imaging of intravoxel incoherent motions: application to diffusion and perfusion in neurologic disorders. *Radiology*. 1986;161:401–407.
8. Moseley ME, Kucharczyk J, Mintorovitch J, Cohen Y, Kurhanewicz J, Derugin N, Asgari H, Norman D. Diffusion-weighted MR imaging of acute stroke: correlation with T2-weighted and magnetic susceptibility-enhanced MR imaging in cats. *AJNR Am J Neuroradiol*. 1990;11:423–429.
9. Schlaug G, Siewert B, Benfield A, Edelman RR, Warach S. Time course of the apparent diffusion coefficient (ADC) abnormality in human stroke. *Neurology*. 1997;49:113–119.
10. Reith W, Hasegawa Y, Latour LL, Dardzinski BJ, Sotak CH, Fisher M. Multislice diffusion mapping for 3-D evolution of cerebral ischemia in a rat stroke model. *Neurology*. 1995;45:172–177.
11. Villringer A, Rosen BR, Belliveau JW, Ackerman JL, Lauffer RB, Buxton RB, Chao YS, Wedeen VJ, Brady TJ. Dynamic imaging with lanthanide chelates in normal brain: contrast due to magnetic susceptibility effects. *Magn Reson Med*. 1988;6:164–174.
12. Belliveau JW, Rosen BR, Kantor HL, Rzedzian RR, Kennedy DN, McKinstry RC, Vevea JM, Cohen MS, Pykett IL, Brady TJ. Functional cerebral imaging by susceptibility-contrast NMR. *Magn Reson Med*. 1990;14:538–546.
13. Ostergaard L, Weisskoff RM, Chesler DA, Gyldensted C, Rosen BR. High resolution measurement of cerebral blood flow using intravascular tracer bolus passages, part I: mathematical approach and statistical analysis. *Magn Reson Med*. 1996;36:715–725.
14. Ostergaard L, Sorensen AG, Kwong KK, Weisskoff RM, Gyldensted C, Rosen BR. High resolution measurement of cerebral blood flow using intravascular tracer bolus passages, part II: experimental comparison and preliminary results. *Magn Reson Med*. 1996;36:726–736.
15. Holman BL, Devous MD Sr. Functional brain SPECT: the emergence of a powerful clinical method. *J Nucl Med*. 1992;33:1888–1904.
16. Patel MR, Edelman RR, Warach S. Detection of hyperacute primary intraparenchymal hemorrhage by magnetic resonance imaging. *Stroke*. 1996;27:2321–2324.
17. Schellinger PD, Jansen O, Fiebich JB, Hacke W, Sartor K. A standardized MRI stroke protocol: comparison with CT in hyperacute intracerebral hemorrhage. *Stroke*. 1999;30:765–768.
18. Astrup J, Siesjo BK, Symon L. Thresholds in cerebral ischemia: the ischemic penumbra. *Stroke*. 1981;12:723–725.
19. Scharbrough F, Messick J Jr, Sundt T Jr. Correlation of continuous electroencephalograms with cerebral blood flow measurements during carotid endarterectomy. *Stroke*. 1973;4:674–683.
20. Hacke W, Kaste M, Fieschi C, von Kummer R, Davalos A, Meier D, Larrue V, Bluhmki E, Davis S, Donnan G, Schneider D, Diez-Tejedor E, Trouillas P, for the Second European-Australasian Acute Stroke Study Investigators. Randomised double-blind placebo-controlled trial of thrombolytic therapy with intravenous alteplase in acute ischaemic stroke (ECASS II). *Lancet*. 1998;352:1245–1251.
21. Holman BL, Hellman RL, Goldsmith SJ, Mena IG, Leveille J, Gherardi PG, Moretti JL, Bischof-Delaloye A, Hill TC, Rigo PM, van Heertum RL, Ell PJ, Buell U, de Roo MC, Morgan RA. Biodistribution, dosimetry, and clinical evaluation of technetium-99 m ethyl cysteinate dimer in normal subjects and in patients with chronic cerebral infarction. *J Nucl Med*. 1989;30:1018–1024.
22. Kuikka JT, Tenhunen-Eskelinen M, Jurvelin J, Kiiliäinen H. Physical performance of the Siemens MultiSPECT 3 gamma camera. *Nucl Med Commun*. 1993;14:490–497.
23. van Gelderen P, de Vleeschouwer MH, DesPres D, Pekar J, van Zijl PC, Moonen CT. Water diffusion and acute stroke. *Magn Reson Med*. 1994;31:154–163.
24. Ulug AM, Beauchamp N Jr, Bryan RN, van Zijl PC. Absolute quantitation of diffusion constants in human stroke. *Stroke*. 1997;28:483–490.
25. Fisel CR, Ackerman JL, Buxton RB, Garrido L, Belliveau JW, Rosen BR, Brady TJ. MR contrast due to microscopically heterogeneous magnetic susceptibility: numerical simulations and applications to cerebral physiology. *Magn Reson Med*. 1991;17:336–347.
26. Weisskoff RM, Zuo CS, Boxerman JL, Rosen BR. Microscopic susceptibility variation and transverse relaxation: theory and experiment. *Magn Reson Med*. 1994;31:601–610.
27. Brott T, Adams HP Jr, Olinger CP, Marler JR, Barsan WG, Biller J, Spilker J, Holleran R, Eberle R, Hertzberg V. Measurements of acute cerebral infarction: a clinical examination scale. *Stroke*. 1989;20:864–870.
28. Lutsep HL, Albers GW, DeCrespigny A, Kamat GN, Marks MP, Moseley ME. Clinical utility of diffusion-weighted magnetic resonance imaging in the assessment of ischemic stroke. *Ann Neurol*. 1997;41:574–580.
29. Lovblad KO, Laubach HJ, Baird AE, Curtin F, Schlaug G, Edelman RR, Warach S. Clinical experience with diffusion-weighted MR in patients with acute stroke. *AJNR Am J Neuroradiol*. 1998;19:1061–1066.
30. Minematsu K, Li L, Sotak CH, Davis MA, Fisher M. Reversible focal ischemic injury demonstrated by diffusion-weighted magnetic resonance imaging in rats. *Stroke*. 1992;23:1304–1310.
31. Baird AE, Warach S. Magnetic resonance imaging of acute stroke. *J Cereb Blood Flow Metab*. 1998;18:583–609.
32. Warach S, Wielopolski P, Edelman RR. Identification and characterization of the ischemic penumbra of acute human stroke using echo planar diffusion and perfusion imaging. *Proc Soc Magn Reson Med*. 1993;1:249. Abstract.
33. Marks MP, de Crespigny A, Lentz D, Enzmann DR, Albers GW, Moseley ME. Acute and chronic stroke: navigated spin-echo diffusion-weighted MR imaging. *Radiology*. 1996;199:403–408.
34. Sorensen AG, Buonanno FS, Gonzalez RG, Schwamm LH, Lev MH, Huang-Hellinger FR, Reese TG, Weisskoff RM, Davis TL, Suwanwela N, Can U, Moreira JA, Copen WA, Look RB, Finklestein SP, Rosen BR, Koroshetz WJ. Hyperacute stroke: evaluation with combined multisection diffusion-weighted and hemodynamically weighted echo-planar MR imaging. *Radiology*. 1996;199:391–401.
35. Warach S, Dashe JF, Edelman RR. Clinical outcome in ischemic stroke predicted by early diffusion-weighted and perfusion magnetic resonance imaging: a preliminary analysis. *J Cereb Blood Flow Metab*. 1996;16:53–59.
36. Baird AE, Benfield A, Schlaug G, Siewert B, Lovblad KO, Edelman RR, Warach S. Enlargement of human cerebral ischemic lesion volumes measured by diffusion-weighted magnetic resonance imaging. *Ann Neurol*. 1997;41:581–589.
37. Rordorf G, Koroshetz WJ, Copen WA, Cramer SC, Schaefer PW, Budzik RF Jr, Schwamm LH, Buonanno F, Sorensen AG, Gonzalez G. Regional ischemia and ischemic injury in patients with acute middle cerebral artery stroke as defined by early diffusion-weighted and perfusion-weighted MRI. *Stroke*. 1998;29:939–943.
38. Tong DC, Yenari MA, Albers GW, O'Brien M, Marks MP, Moseley ME. Correlation of perfusion- and diffusion-weighted MRI with NIHSS score in acute (<6.5 hour) ischemic stroke. *Neurology*. 1998;50:864–870.
39. Barber PA, Darby DG, Desmond PM, Yang Q, Gerraty RP, Jolley D, Donnan GA, Tress BM, Davis SM. Prediction of stroke outcome with echoplanar perfusion- and diffusion-weighted MRI. *Neurology*. 1998;51:418–426.
40. Beauchamp NJ Jr, Bryan RN. Acute cerebral ischemic infarction: a pathophysiologic review and radiologic perspective. *AJR Am J Roentgenol*. 1998;171:73–84.
41. Baron JC, von Kummer R, del Zoppo GJ. Treatment of acute ischemic stroke: challenging the concept of a rigid and universal time window. *Stroke*. 1995;26:2219–2221.



## Combined Diffusion and Perfusion MRI With Correlation to Single-Photon Emission CT in Acute Ischemic Stroke: Ischemic Penumbra Predicts Infarct Growth

Jari O. Karonen, Ritva L. Vanninen, Yawu Liu, Leif Østergaard, Jyrki T. Kuikka, Juh Nuutinen, Esko J. Vanninen, P. L. Kaarina Partanen, Pauli A. Vainio, Katja Korhonen, Jussi Perkiö, Reina Roivainen, Juhani Sivenius and Hannu J. Aronen

*Stroke*. 1999;30:1583-1590

doi: 10.1161/01.STR.30.8.1583

*Stroke* is published by the American Heart Association, 7272 Greenville Avenue, Dallas, TX 75231

Copyright © 1999 American Heart Association, Inc. All rights reserved.

Print ISSN: 0039-2499. Online ISSN: 1524-4628

The online version of this article, along with updated information and services, is located on the World Wide Web at:

<http://stroke.ahajournals.org/content/30/8/1583>

**Permissions:** Requests for permissions to reproduce figures, tables, or portions of articles originally published in *Stroke* can be obtained via RightsLink, a service of the Copyright Clearance Center, not the Editorial Office. Once the online version of the published article for which permission is being requested is located, click Request Permissions in the middle column of the Web page under Services. Further information about this process is available in the [Permissions and Rights Question and Answer](#) document.

**Reprints:** Information about reprints can be found online at:  
<http://www.lww.com/reprints>

**Subscriptions:** Information about subscribing to *Stroke* is online at:  
<http://stroke.ahajournals.org/subscriptions/>